Pharmacogn. Res., 2027; 19(1):348-355.
https://www.phcogres.com

Original Article

Anticancer Effects of *Schinus molle*-Synthesized Iron Nanoparticles in Human HeLa Cervical Cancer Cells

Pavithra Ramamoorthy[1], Ruban Chakravarthy K M[1], Logeshwaran S[1], Vimal S[1,*], Mohamed Saleem T S[2]

[1]Department of Biochemistry, Saveetha Medical College and Hospital, Saveetha Institute of Medical and Technical Sciences (SIMATS), Tamil Nadu, INDIA.
[2]Department of Pharmacy, College of Pharmacy, Nursing and Medical Sciences, Riyadh ELM University, Riyadh, SAUDI ARABIA.

ABSTRACT

Objectives: Green development of iron nanoparticles by plant derived extracts has collected important scientific attention due to their eco-friendly fabrication, cost-effectiveness, and enhanced biological activities. **Materials and Methods:** The current research was assumed to evaluate the anticancer efficacy of Iron Nanoparticles (FeNPs) biosynthesized from leaf extraction of *S. molle* against Human cervical cancer (HeLa) cells through FTIR characterization, MTT cytotoxicity assay and (AO/EtBr) dual-staining methodology. Iron nanoparticles were developed employing Ferric Chloride ($FeCl_3$) as the indication salt in mixture with *S. molle* extract as the bio dropping agent. Physicochemical characterization was achieved via Fourier Transform Infrared Spectroscopy (FTIR). **Results:** Cytotoxic potential was evaluated through the MTT assay at different concentration ranging from 0 to 100 µg/mL. Morphological alterations and apoptotic cell death were observed employing fluorescence microscopy with AO/EtBr dual staining. FTIR spectral analysis revealed characteristic absorption bands at 3378 cm^{-1}, 1634 cm^{-1} and 1087 cm^{-1} confirming the occurrence of hydroxyl, carbonyl and C-O functional groups involved in nanoparticle stabilization. **Conclusion:** MTT assay demonstrated concentration dependent cytotoxicity with cell viability declining from 97.8±2.3% in untreated controls to 23.1±1.8% at 100 µg/mL, yielding an IC_{50} value of approximately 5 µg/mL. AO/EtBr staining revealed clear morphological features of apoptosis as well as chromatin condensation, nuclear fragmentation, and the formation of apoptotic bodies in treated cells relative to untreated controls. The green synthesised FeNPs established potent and dose dependent anticancer activity against HeLa cells initially mediated through induction of apoptotic cell death. These finding suggests that *S. molle*-synthesized FeNPs found promising for further preclinical and clinical evaluation as novel anticancer therapeutic agents.

Keywords: Anticancer Activity, Green Synthesised Iron Nanoparticle, Hela Cells, MTT Assay, *S. molle*.

Correspondence:
Dr. Vimal S
Department of Biochemistry, Saveetha Medical College and Hospital, Saveetha Institute of Medical and Technical Sciences (SIMATS), Chennai-600077, Tamil Nadu, INDIA.
Email: vimals.smc@saveetha.com

Received: 21-04-2026;
Revised: 18-05-2026;
Accepted: 08-07-2026.

INTRODUCTION

Cancer denotes the most difficult universal health challenges of the 21st century place as the 2nd leading cause of death worldwide with an estimated 19.3 million new cases and 10 million cancer associated losses reported in 2020 (Sung *et al.*, 2021). Cervical cancer is a malignancy of hematopoietic tissue characterized by uncontrolled proliferation of immature blood cell precursors constitutes a significant proportion of blood related cancers with considerable morbidity and mortality across all demographic groups (Choi *et al.*, 2024). Conventional therapeutic modalities including chemotherapy, radiotherapy and surgical while clinically active to variable degrees are regularly associated with severe systemic toxicity, multi-drug resistance and adverse side effect profiles that consider ably reduce quality of life for patient. (Magno *et al.*, 2024). So, the imperative to develop fresh, selectively cytotoxic and biocompatible anticancer agents has intensified substantially within the oncologic research community (Basak *et al.*, 2021). In biomedical applications NPs have been generally discovered for drug delivery, diagnostics, imaging, and therapeutic purposes due to their ability to penetrate biological barriers, improve drug solubility, and enable controlled and targeted release (Jaganmoorthy *et al.*, 2026). The size, shape and surface charge of nanoparticles can be personalized to optimize cellular uptake and therapeutic efficacy while their surfaces can be functionalized with biomolecules to improve specificity to cancer cells and decrease damage to normal tissues (Anandachockalingam *et al.*, 2024). Nanotechnology has developed as a transformative discipline within biomedical research, offering extraordinary opportunities for targeted drug delivery system, diagnostic imaging, and direct therapeutic

OPEN ACCESS

Manuscript TECHNOMEDIA

DOI: 10.5530/pres.20270206

intervention at the cellular and molecular level (Ishaque *et al.*, 2025). Green development of nanoparticles using herbal extracts has earned high interest as an environmentally friendly, profitable and maintainable another to conservative chemical and physical methods (Lintao and Medina *et al.*, 2021). Plant based synthesis removes the use of toxic reagents and provides natural dropping and stabilizing agents, enhancing the biocompatibility of the nanoparticles (Baskar *et al.*, 2025). Among the varied of nanomaterials below examination metal oxide nanoparticles have gaining attention significant scientific attention to their distinctive physicochemical properties (Khalil *et al.*, 2017). Iron Nanoparticles (FeNPs) in particular have been widely studied in oncologic backgrounds due to their magnetic characteristic demonstrated biocompatibility and volume to produce Reactive Oxygen Species (ROS) within malignant cells through Fenton type reactions thereby inducing oxidative stress mediated cytotoxicity (Limo *et al.*, 2018). The plant based of nanoparticles applying phytochemical extracts has produced substantial momentum as an ecologically sustainable and economically viable another to conventional chemical and physical fabrication methodologies (Osman *et al.*, 2024). Phytoderived reducing agents comprising a complex matrix of polyphenols, flavonoids, terpenoids, alkaloids and organic acids facilitate the decrease of metallic ions and simultaneously function as capping and stabilizing agents thereby obviating the requirement for hazardous chemical reducing agent and minimizing toxic byproduct generation (Singh *et al.*, 2023). The nanoparticles developed by the help of photosynthesis moreover exhibit synergistic biological activities attributable to the retention of bioactive phytochemical ligands on surface of the particles. *Schinus molle* L., commonly selected as the Peruvian peppertree or pink pepper is a xerophytic aromatic tree distributed across tropical and subtropical regions of South America subsequently naturalized across Africa, Asia and the Mediterranean basin (El-Nashar *et al.*, 2022). The species has been extensively employed in indigenous and traditional medical systems for the treatment of antimicrobial infections, inflammatory conditions, dental caries, respiratory ailments and skin disorders (Fonseca and Huerta-Reyes *et al.*, 2025). Phytochemical study has documented an extraordinarily diverse secondary metabolite profile encompassing essential oil constituents pentacyclic triterpenoids, flavonoids, tannins, phenolic acids and alkaloids many of which possess demonstrated antioxidant, antimicrobial, anti-inflammatory and antiproliferative activities (Radice *et al.*, 2026). The rich polyphenolic and flavonoid content of *S. molle* renders its water extract particularly suitable as a bio decreasing and capping agent for nanoparticle synthesis (Acharya *et al.*, 2025). The current investigation was designed to investigate the anticancer potential of FeNPs biosynthesized from *S. molle* leaf aqueous extract against HeLa cells. Specifically, the objectives encompassed (i) Physicochemical characterization of synthesized FeNPs through FTIR spectroscopy to identify functional groups mediating nanoparticle stabilization (ii) Quantitative assessment of cytotoxic activity through the MTT cell viability assay across a defined concentration gradient (iii) Qualitative visualization of cellular morphological alterations and apoptosis induction employing Acridine Orange/Ethidium Bromide dual-fluorescence staining methodology and (iv) Evaluation of the morphological integrity of HeLa cells at the IC_{50} concentration through phase-contrast microscopy.

MATERIALS AND METHODS

Plant Material Collection and Extract Preparation

S. molle leaves were collected and washed with tap water to remove all unwanted residues and material. After washing the leaves were spread in a shaded place and allowed to dry naturally at room temperature until they become completely dry. After drying the material was crushed manually and powdered using a clean grinder to obtain a fine texture. 10 g of the plant powdered material was placed into a beaker filled with distilled water. The mixture was heated slowly at a mild temperature to allow the bioactive compound to leach into the solvent. After heating the extract was left undisturbed to cool naturally. The cooled mixture was filtered through Whatman filter paper to remove solid residues. Clear extract was collected and kept at 4°C for further process in the development of nanoparticles (Sarwar *et al.*, 2025).

Biosynthesis of Iron Nanoparticles

Iron nanoparticles were developed through 0.1 molarity water solution of ferric chloride hexahydrate ($FeCl_3 \cdot 6H_2O$) was freshly prepared with distilled water. The mixture was accrued by adding 10 mL of *S. molle* leaf extract add dropwise 90 mL of the $FeCl_3$ solution under continuous stirring at 60°C. The preparation of FeNPs was showed by a changing of colour from pale yellow to dark brown black within half an hour of reaction beginning, denoting the reduction of Fe^{3+} ions and nucleation of iron nanoparticles. The combination was kept below stirring for 2 hr at 60°C for complete reaction. The suspension was transfer to centrifugation at 10,000 rpm for 20 min at 4°C and the pellet was washed three times with distilled water followed by ethanol to remove residual phytochemicals and unreacted precursors. The nanoparticle which is purified and the pellet was dried in a hot-air oven at 60°C for 12 hr and stored in airtight container under room temperature for further studies (Elkhateeb *et al.*, 2024).

Fourier Transform Infrared Spectroscopy (FTIR)

Fourier-transform infrared spectroscopy (Nicolet 5700, Thermo Scientific) was used to clarify the of *Schinus molle* green synthesized Iron Nanoparticles. The KBr pellet method was used to develop the samples, which were then analysed over 500-4000 cm^{-1}. The observed vibration bands confirmed that the nanoparticles were synthesised successfully and that bio-based compounds were present on their surface (Viswanathan *et al.*, 2025).

Surface Morphology using SEM

S. molle developed Iron Nanoparticles (FeNPs) were detected using SEM (JEOL JSM5600LV, Japan). The Nanoparticles was spread on polycarbonate sheets and dried using CO_2 critical point drying method to eliminate the remaining moisture. The sample were covered with tinny layer of gold to increase conductivity at before taking picture. The SEM images are possible to get the overall shape, size range and surface morphology of the particles giving a clear idea about their overall formation (Sankar *et al.*, 2026).

Drug Release Study

For Drug release study nanoparticle formulation was dissolved in 10 mL of phosphate buffered saline. The samples were kept incubation at 37°C under continuous shaking at 100 rpm. At fixed time intervals of 1, 3, 5 and 24 hr, supernatant which is 1 mL was withdrawn and centrifuged at 9,000 rpm for 5 min (Thompson *et al.*, 2024; Iani *et al.*, 2023). An equivalent volume of new buffer was added back to maintain the total volume. Calculation of cumulative percentage of extract released from the nanoparticles was using the following equation:

$$(\text{Drug Released at Time (t)} / \text{ Total Drug Content}) \times 100$$

Cell Culture Maintenance

HeLa cell line was obtained from the National Centre for Cell Science (NCCS), Pune, India, and maintained under standard culture conditions in Dulbecco's Modified Eagle's Medium (HiMedia, India) added with 10% (v/v) heat-inactivated fetal bovine serum, 100 U/mL penicillin, 100 µg/mL streptomycin, and 0.25 µg/mL amphotericin B (antibiotic-antimycotic solution. Cell cultures were kept in a humidified CO_2 incubator at 37°C with 5% CO_2 atmosphere. Sub-cultivation was performed every 48-72 hr upon attainment of 70-80% confluency utilizing 0.25% trypsin-EDTA solution. All experimental measures were conducted utilizing cells growth phase (passages 5-15) and all manipulations were performed under aseptic conditions within a biological safety cabinet (Gati *et al.*, 2025).

MTT Cell Viability Assay

Nanoparticle induced cytotoxicity was quantified by MTT assay. Cells seeded (1×10^4/well) in 96-well plates were visible to graded nanoparticle concentrations for 2 days. Post incubation with MTT (0.5 µg/mL, PBS) formazan crystals were solubilized and absorbance was observed at 570 nm. Cell viability percentages were derived accordingly (Paladini *et al.*, 2025).

$$\text{Cell viability (\%)} = (\text{(OD of treated sample)} / \text{(OD of control)}) \times 100$$

Morphological Evaluation of HeLa Cells by Phase-Contrast Microscopy

Phase contrast microscopic test of HeLa cell morphology was assumed to assess treatment induced cytological alterations. HeLa cells were sowed in 6-well culture plates at a density of 3×10^4 cells per well in 2 mL of whole DMEM and incubated for 24 hr to establish adherent monolayers (He *et al.*, 2022).

Acridine Orange/Ethidium Bromide (AO/EtBr) Dual-Fluorescence Staining

HeLa cells were cultured in 6-well plates, treated with FeNPs at the IC_{50} concentration for 24 hr and then harvested by trypsinization. Cell suspensions (1×10^4 cells/mL) were prepared in PBS and stained with a freshly prepared AO/EtBr dual dye solution (1:1 v/v combination of 100 µg/mL AO and 100 µg/mL EtBr in PBS) at a ratio of 9:1 (cell suspension: staining solution). Stained cell suspensions (10 µL) were immediately mounted on clean microscopy slides under coverslips and examined under a fluorescence microscope (Alassiri *et al.*, 2025).

Statistical Analysis

Statistical analysis was performed using GraphPad Prism 14.2 and Origin Pro 2025b. Data are presented as Mean±Standard Deviation (SD) of at least three independent experiments. Differences among multiple groups were evaluated using One-Way Analysis of Variance (ANOVA) followed by Tukey's *post hoc* test.

RESULTS

FTIR Spectroscopic Characterization of Biosynthesized FeNPs

Fourier Transform Infrared Spectroscopic analysis of FeNPs was completed to elucidate the nature of functional groups connected with the surface of green produced FeNPs and to classify the phytochemical responsible for nanoparticle decrease, capping and steadying. The FTIR spectrum of *S. molle* synthesized FeNPs, Figure 1 shows some prominent absorption bands distributed across the midinfrared spectral region (4000-500 cm^{-1}) each corresponding to specific molecular vibrations of surface bound green functional groups. Table 1 showing characteristic absorption bands at 3378 cm^{-1} (O-H stretching), 1634 cm^{-1} (C=O stretching) and 1087 cm^{-1} (C-O stretching). Revealed in Figure 2A and Table 1 of surface bound phytochemical capping agents.

SEM Image of Iron Nanoparticles

SEM analysis image revealed that *Schinus molle*-Synthesized Iron Nanoparticles highly, irregularly clustered morphology of the nanoparticles. The surface presents rough with densely packed granule like formation. The particle size distribution in the image 124 nm to 159 nm result are shown in Figure 2B. Confirming

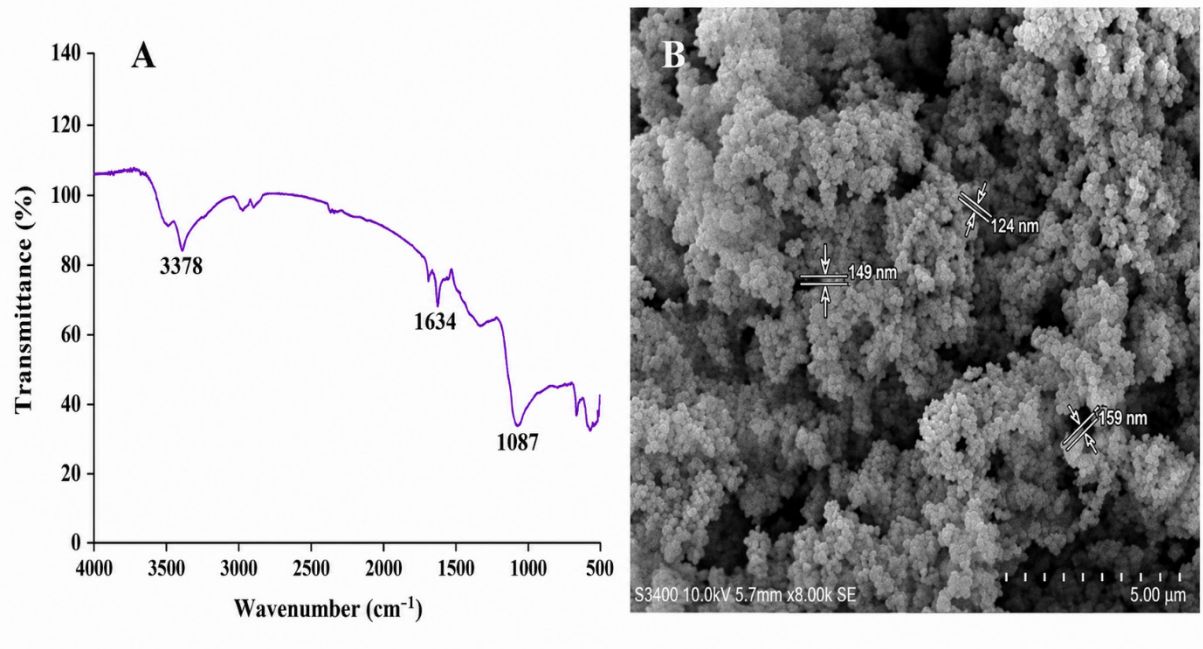

Figure 1: (A) FTIR spectrum of *S. molle d*eveloped Iron Nanoparticles (FeNPs). (B) SEM image of *Schinus molle*-Synthesized Iron Nanoparticles.

Table 1: FTIR spectral band assignments for *Schinus molle*-synthesized iron nanoparticles.

Wavenumber (cm^{-1})	Vibrational Assignment	Possible Phytochemical Origin
3378	O-H stretching (broad)	Polyphenols, Flavonoids, Adsorbed Water
1634	C=O stretching / Amide I	Ketones, Carboxylic Acids, Proteins
1087	C-O stretching	Polysaccharides, Terpenoids, Esters

the formation of nanoparticles within the nanoscale range. The particles show a tendency to clustered which may be due to high surface energy and possible interaction between functional groups. Complete the nanoparticle morphology suggests successful nanoparticle formation with a non-uniform, grouped structure which can be beneficial for applications requiring high surface area for drug delivery and catalytic activity.

In vitro Drug release and Cytotoxicity Assessment MTT Assay

In vitro cumulative release profile of *Schinus molle*-Synthesized Iron Nanoparticles shows a quick initial release within 5 hr and constant release up to 24 hr approaching nearly 100% cumulative release. The drug release from *Schinus molle*-Synthesized Iron Nanoparticles was tested under controlled conditions and the result are shown in Figure 3A. At starting its was a slow drug release. Nearly 50% of drug was released at 300 min it was a sustainable release. which shows the diffusion of drug molecules from the nanoparticles. So, after 1400 min it shows 70% of drastic release of drug form the nanoparticle.

The cytotoxic possible of bio synthesised FeNPs against HeLa cells was assessed over a different concentration range of 0-100 µg/mL following 24 hr of treatment. The MTT assay results are shown in Figures 3B-3D established pronounced concentration dependent reduction in HeLa cell viability with statistically significant differences observed between all treatment groups relative to the untreated control ($p<0.001$ for all comparisons by ANOVA with Tukey's *post hoc* test). Untreated control cells maintained more viability of 97.8±2.3% consistent with normal proliferative activity. Treatment with FeNPs at 5 µg/mL resulted in a marked reduction in cell viability to 49.7±3.1% representing an approximate 49% low relative to untreated controls. Progressive growth in FeNPs different concentration to 10, 25, 50 and 100 µg/mL developed corresponding viabilities of 39.2±2.8%, 31.6±1.9%, 25.3±2.2% and 23.1±1.8% respectively demonstrating a consistent inverse dose-response relationship. The IC_{50} value defined as the concentration of FeNPs inhibiting 50% of cellular metabolic activity relative to the untreated control was determined to be approximately 5 µg/mL representative potent anticancer activity at low concentrations. The initial rejected in cell viability different ranging between 0 and 5 µg/mL followed by a more gradual at highest concentrations suggests a biphasic cytotoxic mechanism potentially building both direct cellular interactions and indirect ROS mediated pathways.

Cell Morphology

Phase-contrast microscopic study of HeLa cell monolayers providing qualitative assessment of FeNP induced morphological

alterations at the IC_{50} concentration. Untreated control cells (Panel A) showed characteristic HeLa cell morphology showing an adherent, spindle-shaped and polygonal cellular architecture with clearly defined cytoplasmic boundaries, prominent nuclei and extensive intercellular contact consistent with actively proliferating epithelial type cells in confluent monolayer culture. The cells established uniform distribution across the surface of the culture with minute detachment or cellular debris observable in the culture medium. In contrast, HeLa cells screening to FeNPs at the IC_{50} concentration for 24 hr (Panel B) exhibited apparent morphological modifications indicative of cytotoxic stress. Treated cells were demonstrated partial loss of the characteristic spindle shaped morphology with cells appearing more rounded and exhibiting reduced intercellular contact and adhesion. The overall cell density in FeNPs treated wells seemed diminished relative to untreated controls, constant with inhibition of cell proliferation and induction of cell death. These morphological observations support the quantitative MTT assay data proving the cytotoxic activity of green based FeNPs against HeLa cells.

Acridine Orange/Ethidium Bromide (AO/EtBr) Fluorescence Staining Analysis

AO/EtBr double fluorescence staining was lively to illustrate the mode of cell death encouraged by green based FeNPs in HeLa cells and to distinguish viable apoptotic and necrotic cellular populations based on differential membrane integrity and nuclear morphology. Typical fluorescence photomicrographs of AO/EtBr-stained HeLa cells are shown with Panel A depicting AO channel (Green Fluorescence FITC Filter) and Panel B shows the united AO/EtBr overlay (Orange/Red Fluorescence, Texas Red filter) in FeNPs treated cells. Fluorescence microscopic examination revealed distinct differential staining patterns revealing of apoptotic cell death in FeNPs treated HeLa cells. Under AO channel imaging (Panel A, green fluorescence), cells displayed heterogeneous fluorescence intensity with indication of nuclear condensation and irregular chromatin distribution, characterized by bright green fluorescent foci within nuclei indicative of chromatin compaction in early apoptotic cells.

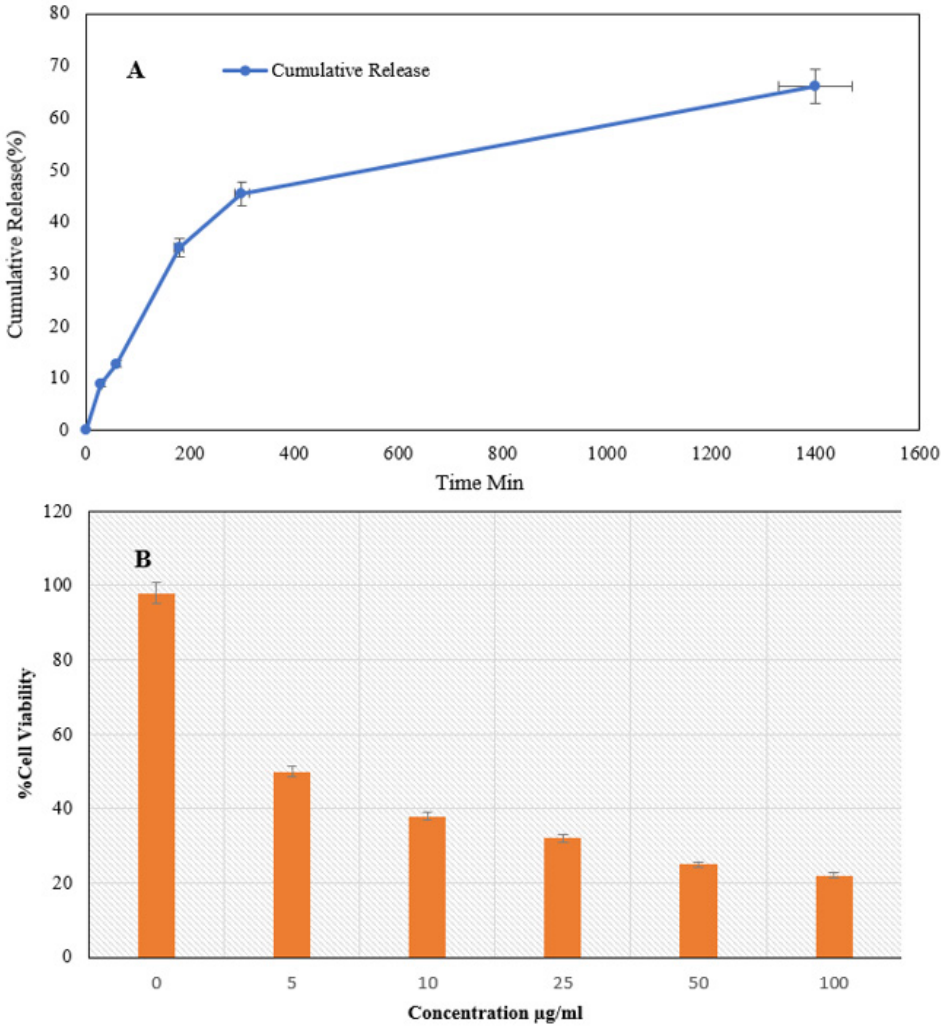

Figure 2: Biological evaluation of *Schinus molle*-synthesized FeNPs. (A) *In vitro* cumulative drug release profile over 24 hr. (B) Cytotoxicity of FeNPs against HeLa cells after 24 hr treatment determined by MTT assay. Data are presented as mean ± SD (*n*=3). Phase-Contrast Microscopic Evaluation of HeLa Cell Morphology.

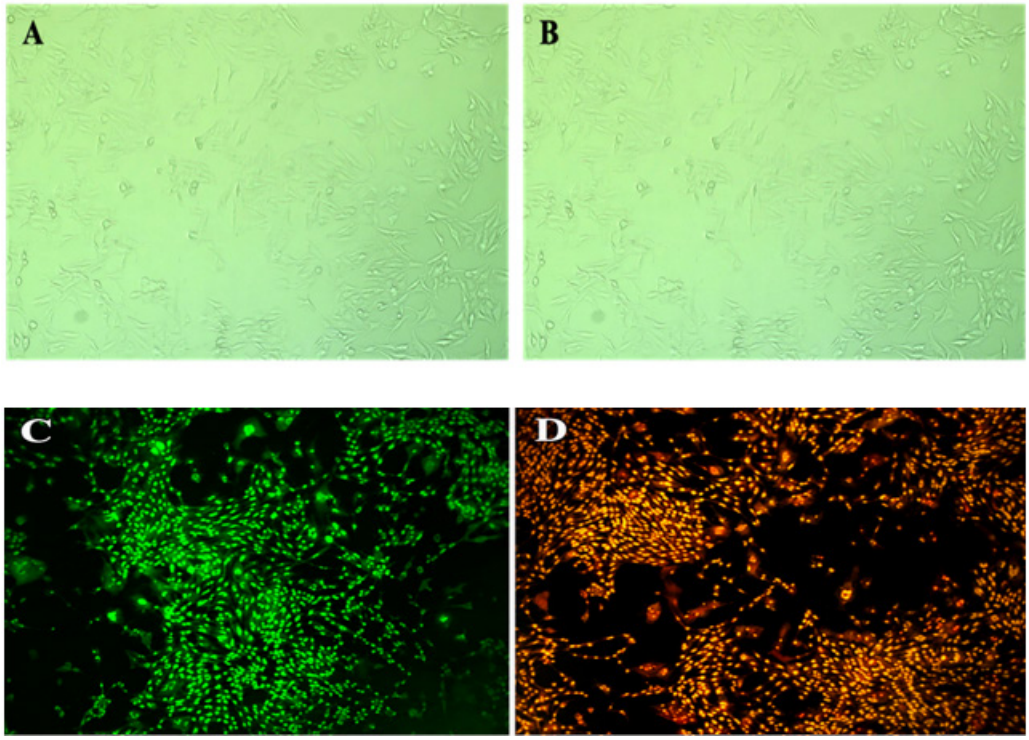

Figure 3: Morphological and apoptotic assessment of HeLa cells treated with *Schinus molle*-synthesized FeNPs. (A) Untreated control cells. (B) Cells treated with FeNPs at IC_{50} (5 µg/mL) for 24 hr showing reduced cell density and morphological changes. (C) AO-stained cells exhibiting green fluorescence of viable cells. (D) AO/EtBr-stained cells showing orange-red fluorescence and nuclear condensation indicative of apoptosis.

The overlay fluorescence micrograph (Panel B) demonstrated the occurrence of cells exhibiting orange-to-red nuclear fluorescence with condensed, fragmented, or crescent-shaped nuclear morphology, characteristic morphological hallmarks of late apoptosis attributed to EtBr intercalation into DNA of cells with compromised membrane integrity. Specifically the following cellular categories were identified (i) Viable cells displaying uniform bright green fluorescence (AO-positive, EtBr-negative) with normal nuclear morphology (ii) Early apoptotic cells exhibiting intense green fluorescence with condensed chromatin distributed in a granular pattern (iii) Late apoptotic cells displaying orange-red fluorescence with nuclear fragmentation and apoptotic body formation and (iv) Rare necrotic cells identified by diffuse orange-red fluorescence with nuclear swelling. The predominant observation of late apoptotic cellular morphology, characterized by membrane blebbing, chromatin condensation and nuclear fragmentation with the development of membrane-enclosed apoptotic bodies in FeNP-treated cells relative to the predominantly viable green-fluorescing cells observed in untreated controls provides compelling evidence that *S. molle*-synthesized FeNPs induce programmed cell death through an apoptotic mechanism in HeLa cells. The elevated proportion of orange/red-fluorescing cells in treated samples relative to controls clearly demonstrates treatment-induced membrane permeabilization characteristic of the late apoptotic stage.

DISCUSSION

The present investigation provides comprehensive indication for the strong *in vitro* anticancer activity of iron nanoparticles synthesised by plant based from *S. molle* leaf aqueous extract against HeLa cells. The integration of physicochemical quantitative cytotoxicity cell characterization, morphological and fluorescence-based apoptosis finding collectively extended mechanistic framework for understanding the antiproliferative and pro-apoptotic effects of the synthesised nanomaterial. FeNP nanoparticles exposed potent antimicrobial possible against certain bacterial strains. In the same way, the amastigote and promastigote forms of the parasite *Leishmania tropica* were existing to be susceptible to the synthesized NPs. antioxidant, ABTS, α-amylase, α-glucosidase, acetylcholinesterase, and butyrylcholine esterase were potently inhibited by these nanoparticles, representative that they could be efficiently used as therapeutic agents for the oxidative stress and linked difficulties, such as diabetes and Alzheimer's (Zafar *et al.*, 2022). In the anticancer examination, the cells given with biosynthesized FeNPs were calculated by MTT assay for 2 days as respects the anti-Human Cholangiocarcinoma and Cytotoxic properties towards normal (HUVEC) and cholangiocarcinoma carcinoma cell lines, i.e. HCM-CSHL-0174-C22, CCLP-1, and QBC939. The IC_{50} values of biosynthesized FeNPs were 196, 237, and 278 µg/mL against HCM-CSHL-0174-C22, CCLP-1, and QBC939 cell lines, respectively. The viability of the cholangiocarcinoma cell

line reduced dose-dependently in the occurrence of FeNPs (Zhao *et al.*, 2022). *S. molle*s are a high cause of secondary metabolites. 13 Gallo tannins, 3 phenolic acids, phenolic acid glucoside, 3 phenolic acid esters, organic acid, Gallo tannin derivative and 9 flavonoids were described and more quantified. Their study revealed that feruloyl tartaric A, a phenolic acid ester was the main phenolic acid while quercetin 3-O-glucuronide and catechin were the major flavonoids, and digalloylshikimic acid B as well as digalloylquinic acid were the leading tannins (Bvenura *et al.*, 2022). No decrease at the 0.1 mg/mL concentration (n=9), the usual signal decrease at 0.5 mg/mL was 6.5 % (n=9, ±=8.0%), and the average signal reduction for the 1 mg/mL concentration was 11.12 % (n=9, ± =10.19%). There was no substantial change among the control cells and the 0.1 mg/mL, or 0.5 mg/mL test cells. The 1 mg/mL signal was found to be significant (p=0.0055). The correction factor determined was applied to the measured values using the formula (Martin *et al.*, 2024). The maximum amount of late apoptotic cells was detected at the 9 µg/mL dose of CO-NPs (*Cinchona officinalis* extract-loaded iron oxide nanoparticles) when compared to COE (*Cinchona Officinalis* Extract). Physical counting of apoptotic and necrotic cells within an average of 300 cells presents with 83% in apoptotic and 6% were present with necrotic morphology (Al-Harbi *et al.*, 2022).

CONCLUSION

The present investigation proves that iron nanoparticles plant-based synthesis from *S. molle* leaf aqueous extract exhibit significant and concentration-dependent anticancer activity against HeLa cells *in vitro*. FTIR spectroscopic characterization confirmed effective phytochemical capping and stabilization of synthesized FeNPs through O-H, C=O, and C-O functional group interactions. MTT cytotoxicity assay conventional an IC_{50} of approximately 5 µg/mL against HeLa cells, with capability of declining progressively to 23.1±1.8% at 100 µg/mL. Phase contrast microscopy validated concentration reliant on morphological changes revealing of cytotoxic stress, whilst AO/EtBr fluorescence staining gives definitive evidence of apoptotic cell death as the initial cytotoxic mechanism, characterized by chromatin condensation, nuclear fragmentation and apoptotic body development. These results cooperatively found green based development of *S. molle* FeNPs as capable anticancer candidates warranting further mechanistic investigation. The exploitation of *S. molle* phytochemicals as green reducing and functionalizing agents represents a convergence of ethnobotanical knowledge and nanotechnology that may contribute to the growth of additional efficacious and smaller toxic anticancer therapeutic modalities.

ACKNOWLEDGEMENT

The corresponding author extends thanks to all co-authors for their contributions to this work. This study was supported by the Department of Biochemistry, Saveetha Medical College and Hospitals, Saveetha Institute of Medical and Technical Sciences, Chennai, Tamil Nadu, India.

ABBREVIATIONS

AO/EtBr: Acridine Orange/Ethidium Bromide; **CO_2:** Carbon Dioxide; **DMEM:** Dulbecco's Modified Eagle Medium; **EtBr:** Ethidium Bromide; **$FeCl_3$:** Ferric Chloride; **FeNPs:** Iron Nanoparticles; **FITC:** Fluorescein Isothiocyanate; **FTIR:** Fourier Transform Infrared Spectroscopy; **HeLa:** Human Cervical Cancer Cell Line; **IC_{50}:** Half-Maximal Inhibitory Concentration; **KBr:** Potassium Bromide; **MTT:** 3-(4,5-Dimethylthiazol-2-yl)-2,5-Diphenyltetrazolium Bromide; **NCCS:** National Centre for Cell Science; **NPs:** Nanoparticles; **O-H:** Hydroxyl Group; **PBS:** Phosphate Buffered Saline; **ROS:** Reactive Oxygen Species; **SEM:** Scanning Electron Microscopy; **SIMATS:** Saveetha Institute of Medical and Technical Sciences; **U/mL:** Units per Milliliter; **µg/mL:** Micrograms per Milliliter, **ANOVA:** Analysis of Variance; **AO:** Acridine Orange; **EDTA:** Ethylenediaminetetraacetic acid; **FBS:** Fetal Bovine Serum; **SD:** Standard Deviation.

CONFLICT OF INTEREST

The authors declare that there is no conflict of interest.

ETHICAL APPROVAL

This study did not involve human participants or animals. Experiments were performed using the commercially available HeLA cell line obtained from NCCS, Pune, India; therefore, ethical approval and informed consent were not required.

SUMMARY

This study details the green synthesis of Iron Nanoparticles (FeNPs) using *Schinus molle* leaf extract, which acted as a reducing and capping agent. Characterization via FTIR and SEM confirmed the formation of functionalized nanoparticles in the 124-159 nm range. The FeNPs exhibited potent, dose-dependent anticancer activity against HeLa cells, achieving an IC_{50} of approximately 5 µg/mL. Qualitative analysis through phase-contrast and fluorescence microscopy confirmed that cell death was mediated via apoptosis, characterized by nuclear fragmentation and the formation of apoptotic bodies.

REFERENCES

Anandachockalingam, A., Shanmugam, R., Ryntathiang, I., *et al.* (2024). Green synthesis of silver nanoparticles using *Zingiber officinale* and *Ocimum gratissimum* formulation for its anti-inflammatory and antidiabetic activity: An in vitro study. Cureus, 16(4).

Acharya, C., Mishra, S., Chaurasia, S. K., *et al.* (2025). Synthesis of metallic nanoparticles using biometabolites: Mechanisms and applications. Biometals, 38(1), 21-54.

Al-Harbi, L. N., Al-Shammari, G. M., Subash-Babu, P., Mohammed, M. A., Alkreadees, R. A., & Yagoub, A. E. A. (2022). *Cinchona officinalis* phytochemicals-loaded iron oxide nanoparticles induce cytotoxicity and stimulate apoptosis in MCF-7 human breast cancer cells. Nanomaterials, 12(19), 3393.

Alassiri, S. (2025). Berberine induces ferroptosis and impairs migration via glutathione peroxidase4/six-transmembrane epithelial antigen of prostate3 signaling pathway in oral cancer cells. The Journal of Contemporary Dental Practice, 26, 1050-1059.

Basak, D., Arrighi, S., Darwiche, Y., & Deb, S. (2022). Comparison of anticancer drug toxicities: Paradigm shift in adverse effect profile. Life, 12(1), Article 48. https://doi.org/10.3390/life12010048https://doi.org/10.3390/life12010048

Baskar, G., Palaniyandi, T., Al-Mutiry, M., *et al.* (2025). Biocatalytic green synthesis of iron oxide nanoparticles using red seaweed *Portieria hornemannii* for biomedical applications. Biocatalysis and Agricultural Biotechnology, 70, 103831.

Bvenura, C., & Kambizi, L. (2022). Composition of phenolic compounds in South African *Schinus molle* L. berries. Foods, 11.

Choi, H.-S., Kim, B. S., Yoon, S., Oh, S.-O., & Lee, D. (2024). Leukemic stem cells and hematological malignancies. International Journal of Molecular Sciences, 25(12), Article 6639. https://doi.org/10.3390/ijms25126639

El-Nashar, H. A. S., Mostafa, N. M., Abd El-Ghffar, E. A., *et al.* (2022). The genus Schinus (Anacardiaceae): A review on phytochemicals and biological aspects. Natural Product Research, 36(18), 4839-4857.

Elkhateeb, O., Atta, M. B., & Mahmoud, E. (2024). Biosynthesis of iron oxide nanoparticles using plant extracts and evaluation of their antibacterial activity. AMB Express, 14(1), 92.

Fonseca, R. M., & Huerta-Reyes, M. (2025). Antidiabetic properties of the tropical tree *Schinus molle* L. (pirul): A comprehensive review. Pharmaceuticals, 18(11).

Gati, J. M., Terefe, E. M., Okanya, P., Bargul, J., & Muriuki, J. (2025). Evaluation of anticancer activity of solvent fractions of *Croton megalocarpus* against human cervical adenocarcinoma cell line (HeLa). Natural Product Communications, 20(3).

He, L., *et al.* (2022). Morphology analysis of unlabeled red blood cells based on quantitative differential phase contrast microscopy. Cytometry Part A, 101(8), 648-657.

Iani, I. (2023). Effect of ethanol water concentration on phenolic composition antioxidant and antimicrobial activities of *Rosmarinus tournefortii* de Noé residues. Journal of Food Measurement and Characterization, 17(2), 1602-1615.

Ishaque, P. I., *et al.* (2025). Convergence at the nanoscale: Transformative advances in drug delivery, vaccinology, and biomedical diagnostics. Scholars Academic Journal of Pharmacy, 14(6), 128-162.

JaganMoorthy, S., Subbarayan Ravichandar, P. R., Ganesan, H., Deepika, B., Durgadevi, P., Arokyapraveen, A., Girigoswami, A., & Girigoswami, K. (2026). Plantain peel extract-mediated synthesis of CuO nanoparticles: Comprehensive characterization, bioinertness *in vitro* and *in vivo*, and anticancer evaluation. ADMET and DMPK, 14, Article 3201. https://doi.org/10.5599/admet.3201

Khalil, M., Jan, B. M., Tong, C. W., *et al.* (2017). Advanced nanomaterials in oil and gas industry: Design, application and challenges. Applied Energy, 191, 287-310.

Limo, M. J., *et al.* (2018). Interactions between metal oxides and biomolecules: From fundamental understanding to applications. Chemical Reviews, 118(22), 11118-11193.

Lintao, R. C. V., & Medina, P. M. B. (2021). Screening for anticancer activity of leaf ethanolic extract of *Alpinia elegans* ("tagbak") on human cancer cell lines. Asian Pacific Journal of Cancer Prevention, 22(12), 3781-3787.

Magno, G. M., Lotilla, G. E., Ambrosio, E. R., Nagera, F. L., Grino, M. I., Castro, M. R., Millan, J. A., Manzano, J. A., Tiongco, R. E., & Albano, P. M. (2024). Blood-based FTIR spectroscopy as a minimally invasive diagnostic method for colorectal cancer: A meta-analysis. Asian Pacific Journal of Cancer Prevention, 25(5), 1487-1495. https://doi.org/10.31557/APJCP.2024.25.5.1487

Martin, L., *et al.* (2024). Determination of the optical interference of iron oxide nanoparticles in fluorometric cytotoxicity assays. Heliyon, 10.

Osman, A. I., *et al.* (2024). Synthesis of green nanoparticles for energy, biomedical, environmental, agricultural, and food applications: A review. Environmental Chemistry Letters, 22(2), 841-887.

Paladini, G., *et al.* (2025). Morphological and physicochemical characterization of single-species bacterial biofilms probed by SEM, FTIR-ATR, and μ-Raman techniques. WSEAS Transactions on Biology and Biomedicine, 22, 214-222.

Radice, M., *et al.* (2026). *Schinus molle* L. essential oil: Chemotypes, bioactive compounds, and pharmaceutical insights: A systematic review. Processes, 14.

Sankar, M., Balaji, M. B., & Sugumar, V. (2026). Green synthesis of ZnO nanoparticles using *Mentha piperita* extract: Enhanced anticancer activity against hepatocellular cancer cells. Next Research, 4, 101211.

Sarwar, K., Nazli, Z. I., Munir, H., Aslam, M., & Khalofah, A. (2025). Biosynthesis of zinc oxide nanoparticles using *Moringa oleifera* leaf extract, probing antibacterial and antioxidant activities. Scientific Reports, 15.

Singh, H., *et al.* (2023). Revisiting the green synthesis of nanoparticles: Uncovering influences of plant extracts as reducing agents for enhanced synthesis efficiency and its biomedical applications. International Journal of Nanomedicine, 4727-4750.

Sung, H., Ferlay, J., Siegel, R. L., Laversanne, M., Soerjomataram, I., Jemal, A., & Bray, F. (2021). Global cancer statistics 2020: GLOBOCAN estimates of incidence and mortality worldwide for 36 cancers in 185 countries. CA: A Cancer Journal for Clinicians, 71(3), 209-249. https://doi.org/10.3322/caac.21660

Thompson, P. T., Boamah, V. E., & Badu, M. (2024). *In vitro* antioxidant, antimicrobial and phytochemical properties of extracts from the pulp and seeds of the African baobab fruit (*Adansonia digitata* L.). Heliyon, 10.

Viswanathan, A., Sajith, S., Harini, M., Mathiyazhagan, S., & Vimal, S. (2025). Development of a *Calophyllum inophyllum*-loaded biodegradable chitosan-PVA hydrogel: A multifunctional platform for HT-29 colon cancer cell and antidiabetic applications. Asian Pacific Journal of Cancer Biology, 10(4), 845-852.

Zafar, S., *et al.* (2022). Development of Iron Nanoparticles (FeNPs) using biomass of Enterobacter: Its characterization, antimicrobial, anti-Alzheimer's, and enzyme inhibition potential. Micromachines, 13.

Zhao, J., Yu, Y., Wang, Y., & Cheng, S. (2022). Green formulation and characterization of Fe nanoparticles containing Calendula extract and investigation of the antioxidant, cytotoxic and anti-human cholangiocarcinoma properties. Archives of Medical Science, 10.

Cite this article: Ramamoorthy P, Ruban Chakravarthy KM, Logeshwaran S, Vimal S, Mohamed Saleem T. Anticancer Effects of *Schinus molle*-Synthesized Iron Nanoparticles in Human HeLa Cervical Cancer Cells. Pharmacog Res. 2027;19(1):348-55.